UNCONVENTIONAL RESERVOIR CHARACTERIZATION BASED ON SPECTRALLY CORRECTED SEISMIC ATTENUATION ESTIMATION

FANGYU LI[1], HUAILAI ZHOU[2], TAO ZHAO[1] and KURT J. MARFURT[1]

[1] *University of Oklahoma, Norman, OK 73019, U.S.A. fangyu.li@ou.edu*
[2] *State Key Laboratory of Oil and Gas Reservoir Geology and Exploration, Chengdu University of Technology, Chengdu, Sichuan 610059, P.R. China.*

(Received March 2, 2016; revised version accepted July 15, 2016)

ABSTRACT

Li, F., Zhou, H., Zhao, T. and Marfurt, K.J., 2016. Unconventional reservoir characterization based on spectrally corrected seismic attenuation estimation. *Journal of Seismic Exploration*, 25: 447-461.

Fracture characterization is critical in exploration and development in unconventional resource plays. Fluid-filled fractures and cracks directly alter the effective impedance of rocks, attenuate amplitude and distort seismic spectrum, all of which make the seismic attenuation estimation a promising tool for characterizing fracture system. However, existing methods for estimating seismic attenuation are usually based on "Constant Q" model, which ignores the interference from reflectivity anomalies. For unconventional reservoirs, the spectrum of the reflected wave may be affected by the presence of thin (shales) beds in the formation, which makes Q estimates less reliable. We employ a non-stationary Q model to characterize attenuation, and correct the reflected spectrum by using inverted reflectivity sequence based on well logs to remove local thin-bed effects from seismic reflection data. In synthetic examples, variance in the estimated values and unphysical negative Q values are reduced sgnificantly. Following the workflow, we also applied attenuation estimation on a seismic survey acquired over the Barnett Shale. The recovered Q estimates have a good correspondence with the production data. Though, the attribute is the average over a target formation, this may be sufficient to find evidence of fluid-filled fractures, or variation in lithology.

KEY WORDS: seismic attenuation estimation, localized spectral correction, time-variant Q model, unconventional reservoir characterization, thin beds.

0963-0651/16/$5.00

INTRODUCTION

Identifying highly fractured zones or sweet spots in naturally fractured reservoirs is important where fractures often act as significant conduits for fluid flow (Burns, 2004). Lynn (2015) reports changes in attenuation as a function of fracture orientation for natural fractures. In addition to fractures, shales are also expected to exhibit strong attenuation associated with microcracks with possibly new loss mechanisms linking attenuation to kerogen maturity and organic content (Lynn and Beckham, 1998). Thus, seismic attenuation may play a crucial role in the exploration and exploitation of unconventional hydrocarbon resources.

Existing basic methods for seismic attenuation, such as the spectral ratio method (Hauge, 1981; White, 1992; Dasgupta and Clark, 1998), the frequency shift methods (Quan and Harris, 1997; Zhang and Ulrych, 2002), measures quality factor Q based on the variance of the seismic wavelet spectra. However, the classic "Constant Q" model ignores the interference from reflectivity anomalies. For unconventional reservoirs, the spectrum of the reflected wave may be affected by the presence of thin beds (shale reservoir) in the formation, which makes Q estimates less reliable.

Hackert and Parra (2004) proposed to use the known reflectivity sequence from a nearby well log to correct the local spectrum. Inspired by their work, and considering unconventional reservoirs, we employ a new Q model to estimate seismic attenuation, and correct the reflected spectrum by removing local thin-bed effects from seismic reflection data, by using well logs to invert seismic impedance volume of the whole survey, and then computing the reflectivity sequence to correct the reflected spectrum. In the synthetic examples, there is significantly less variance in the estimated Q values, and fewer unphysical negative Q values are obtained. We also show a field example from Barnett Shale, with promising result.

TIME-VARIANT SPECTRAL MODEL

When a seismic wave propagates in a viscoelastic medium in a constant linear frequency attenuation model, the apparent Q arises by considering a traveling wave whose spectral amplitude exponentially reduces with travel time as (Aki and Richards, 2002)

$$A(f,t) = S(f)\exp(-\pi ft/Q) \quad , \tag{1}$$

where S(f) is the source wavelet spectrum, t is the traveltime, and A(f,t) is the received signal spectrum including all geometric spreading, source, and receiver effects. In this model, the quality factor Q is constant on all frequencies, so it is called "Constant Q model".

Let us start over from a simple (noise free) convolution model (Sheriff and Geldart, 1995):

$$a(t) = \int_{-\infty}^{\infty} s(t)r(t - \tau)d\tau \quad , \tag{2}$$

where a(t) is the reflected signal, s(t) is the source wavelet, and r(t) is the reflectivity series. In this model, the seismic signal is the convolution of the source wavelet and reflectivity sequence. The frequency expression of this convolution model is

$$A(f) = S(f)R(f) \quad , \tag{3}$$

where, A(f), S(f) and R(f) are the Fourier transforms of the seismic signal, source wavelet, and reflectivity series, respectively. If the medium is attenuating, with constant Q, then the spectrum will be reduced:

$$A(f) = S(f)R(f)exp(-\pi ft/Q) \quad . \tag{4}$$

Compared with eqs. (1) and (4), we can find the Constant Q model ignores the reflection coefficient effects. The reasons are: the reflectivity coefficient is usually viewed as random, so its spectrum is white; the Constant Q model is mainly dealing with one layer, and in common geophysics, we often assume the reflection coefficient only appears at the boundaries of layers, but not within layers. Although, the reflectivity is fairly random at a large scale, the local reflectivity spectrum is not white. What's more, for unconventional reservoirs, such as shale, there are thin layers in the target formation. Thus, we should consider the local reflectivity change, which would distorts seismic spectrum otherwise.

Grossman et al. (2001) introduced a non-stationary convolution model, which is actual a more generalized form of eq. (4), to do the attenuation estimation:

$$A(f,t) = S(f)\alpha(f,t)R(f) \quad , \tag{5}$$

where $\alpha(f,t)$ is the attenuation factor expression in the frequency domain. This formula can also be modified into: [(Grossman et al. (2001) have proved the validity of this transform]

$$A(f,t)/R(f) = S(f)\alpha(f,t) \quad . \tag{6}$$

If we can get the estimation of the local reflectivity coefficient, the interference of local geology can be suppressed, which can lead to a more accurate Q estimation.

LOCALIZED SPECTRAL CORRECTION

Considering there are two local subsets of reflectors $r_1(t)$ and $r_2(t)$ near time t_1 and t_2, respectively. Then, we can express their spectra as:

$$A_1(f,t_1) = S(f)R_1(f)\exp[-\pi f t_1/Q] \ ,$$
$$A_2(f,t_2) = S(f)R_2(f)\exp[-\pi f t_2/Q] \ . \quad (7)$$

Taking the logarithm of their ratio, we have

$$\ln[A_1(f,t_1)/A_2(f,t_2)] = \ln[R_1(f)/R_2(f)] - \pi f(t_1 - t_2)/Q \ . \quad (8)$$

If there is no reflectivity anomaly, the ratio between R_1 and R_2 is independent of frequency, so the first term on the right-hand side is constant, and Q can be estimated form the slope of the log-spectral ratio between A_1 and A_2. But there are usually spectral anomalies, then the first term on the right-hand side varies with frequency, and the spectral slope is not solely related to Q.

Therefore, we need to get rid of the interference from the reflectivity coefficient. When the well-log impedance data are available, we can compute the reflectivity at the well location. In our work, we use known reflectivity sequence in synthetic examples and invert the seismic impedance using well logs in field data examples. Thus, instead of just a few well locations, we can do the localized spectral correction over the whole seismic survey, with promising results.

After getting the reflectivity spectrum, move the first term on the right-hand side of eq. (8) to the left-hand side, and derive R(f):

$$\ln\{[A_1(f,t_1)/R_1(f)]/[A_2(f,t_2)/R_2(f)]\} = -\pi f(t_1 - t_2)/Q \ . \quad (9)$$

Note that $A(f,t)/R(f)$ is a local spectrum correction. Then, we can use Q estimation methods, such as spectral ratio and central frequency shift methods, to get its value.

To sum up, this method has the following steps (the workflow is shown in Fig. 1):

1. Select a reference reflection and some target reflections; in the same time, invert seismic impedance based on known well logs.

2. In order to get the local spectral reflection, the time-frequency transform should be applied in a local (short time window) period. The time window should be short enough to select the reflection of interest but long enough to assure the frequency resolution.

3. Apply the spectral correction to get the corrected spectrum.

4. Use Q estimation methods to compute the Q value.

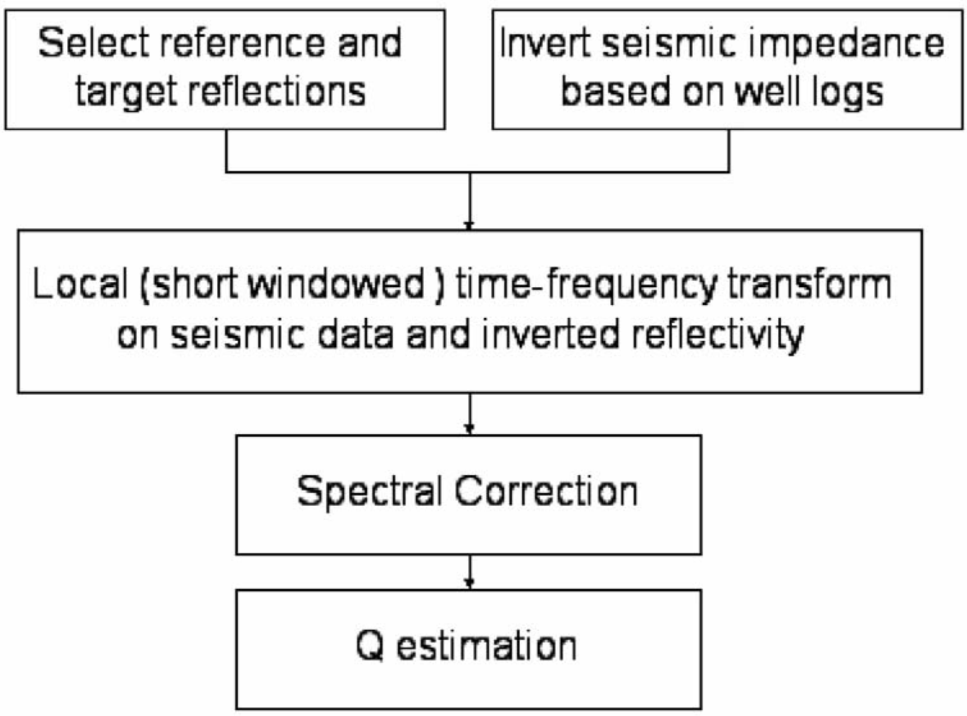

Fig. 1. Workflow of the well-log based local spectral correction Q estimation.

INTERFERENCE FROM ILL-SPACED REFLECTORS

As we know, the reflected data come from the convolution of the source wavelet with the reflectivity series. For a relatively long time range, the reflectivity sequence is usually viewed as random, so it has a white spectrum.

However, the localized reflection spectrum can be distorted by ill-spaced reflectors. Fig. 2 demonstrates the possible interference phenomena. For a single reflector (Fig. 2a), there is no spectral distortion. For the three evenly spaced reflectors shown in Fig. 2c, the reflection spectrum is enhanced near 45 Hz and suppressed near 15 Hz and 75 Hz, which shows that local reflectivity can result in constructive and destructive interference at certain frequencies. Fig.2e shows closely but randomly spaced reflectors, in which the reflected spectrum may be affected irregularly. It could suppress low-frequency content in the combined reflection because of the possible low frequency notches, as in this case, which will give the appearance of negative Q through increased amplitude at high frequencies.

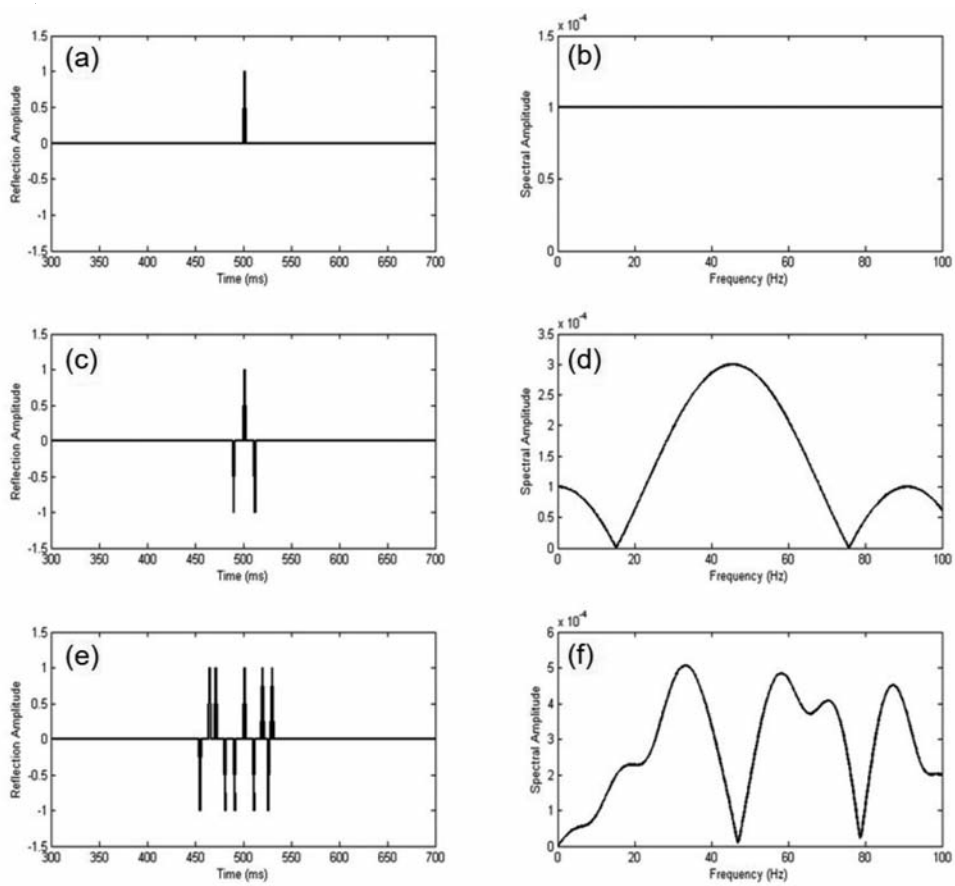

Fig. 2. Three hypothetical spike reflectivity sequences and their corresponding spectra.

SYNTHETIC THIN-BED EXAMPLE

We built a synthetic example consisting of five layers (four reflectors), each with different Q and P-velocity (Fig. 3). The source pulse is a Ricker wavelet of 100-Hz central frequency. We set up two cases on this model: one with no thin beds, and the second case with thin beds added, as shown in Fig.3. From Fig. 2, we can infer that the reflectivity sequences with thin beds are distorted.

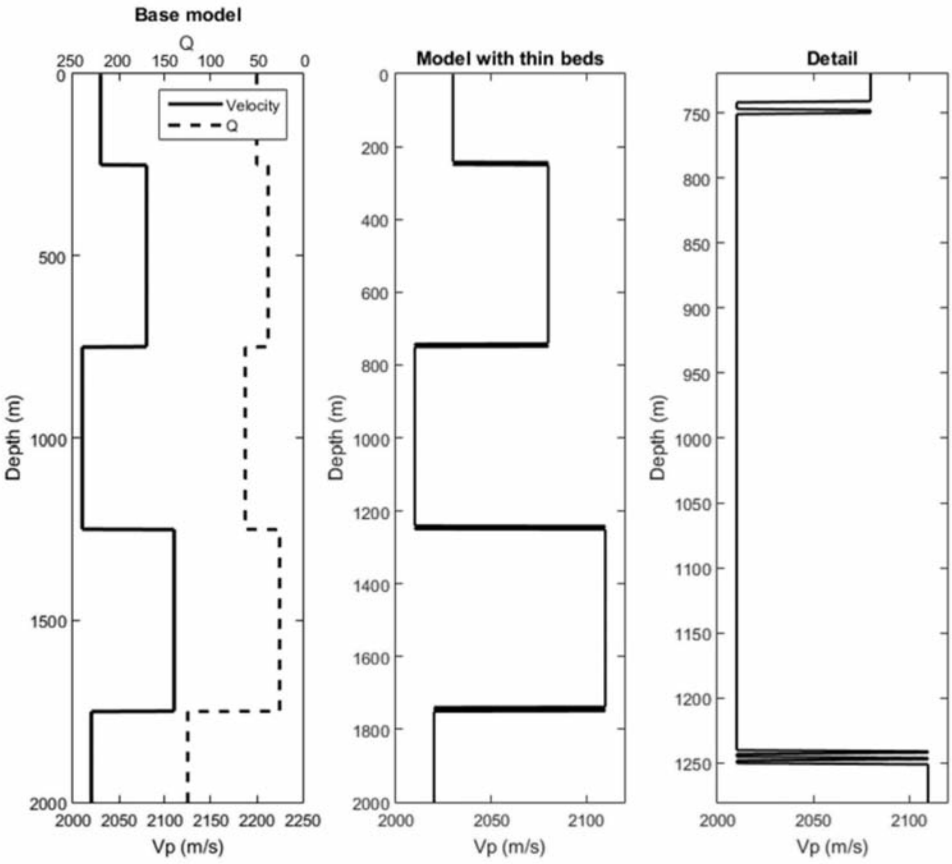

Fig. 3. Velocity models for synthetic seismic reflection data without and with thin beds added.

The uncorrected and corrected normalized local spectra of the four reflections are shown in Fig. 4. The solid curves are the ideal reflected spectra without thin beds, while dashed curves are the uncorrected spectra for reflections including thin beds, and the dotted curves are the spectrum with the local spectral correction. Ideally, the corrected spectrum (dotted curves) would exactly match the ideal spectrum (solid curve). This does not happen because we have smoothed out the zeroes in the spectrum of the reflectivity sequence.

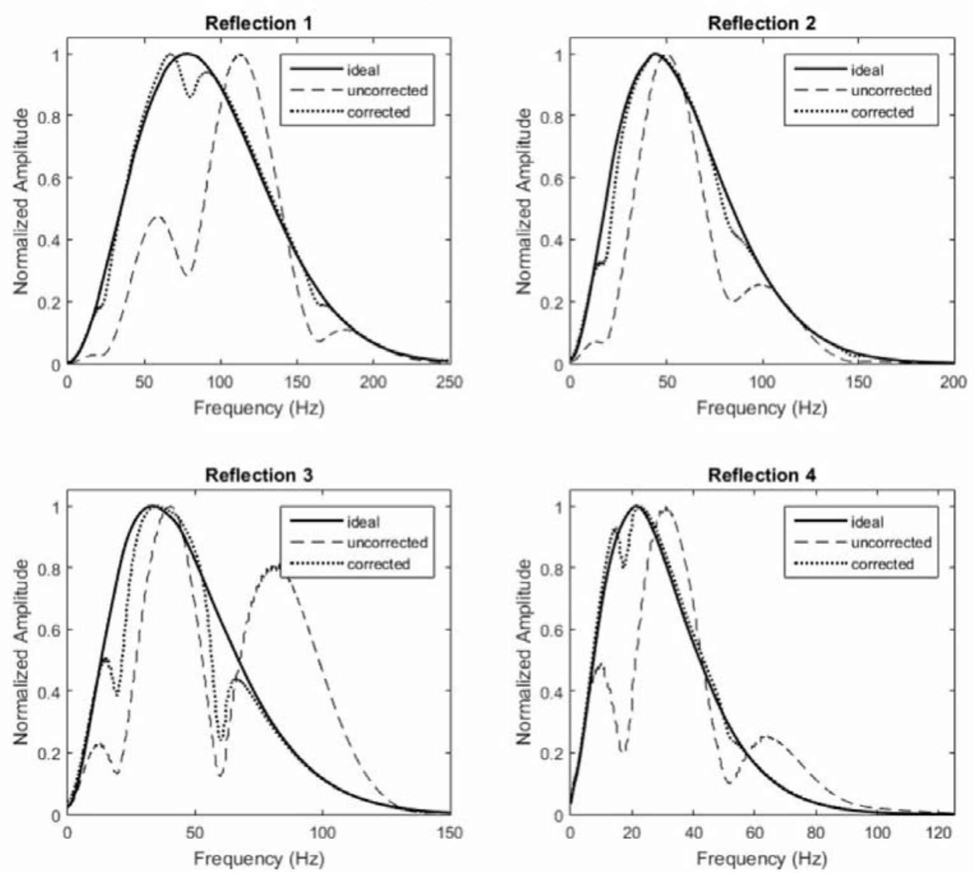

Fig. 4. Comparison between uncorrected and corrected normalized local reflection spectra. In each figure, the solid curve is the spectrum if there are no thin beds. The dashed curve is the spectrum with thin beds. The dotted curve is the corrected spectrum. Note that not all frequency axes span the same range.

The first reflection is the reference and we compute the average Q between that and each later reflection using both the uncorrected and corrected spectra (Table 1). Only the central frequency shift (CFS) method is used. Without thin beds present, the method recovers the Q of each layer almost exactly. The thin beds at layer boundaries in the second model, however, interfere with the reflection spectra in the manner discussed above, so that Q values of the uncorrected CFS method are quite inaccurate. Applying the well-log-based spectral correction substantially removes this effect, and the corrected Q values are of reasonable accuracy.

Table 1. True and computed values of Q from the synthetic test data, for cases of no thin beds and thin beds added. When thin beds are present, Q values are computed with and without the spectral correction technique.

	True Value	Estimation without thin beds	Estimation with thin beds (uncorrected)	Estimation with thin beds (corrected)
Layer 1	40	37.2	81.5	37.9
Layer 2	30	31.2	16.5	31.1
Layer 3	50	47.2	-307	44.6
Layer 4	20	20.6	5	20.4

FIELD DATA APPLICATION

The Barnett Shale is a very important unconventional shale gas system in the Fort Worth Basin (FWB), Texas where it serves as a source rock, seal, and trap (Pérez, 2009). If possible, mapping of fracture patterns could have a significant value in evaluation of the effectiveness of alternative fracking strategy used. The section was deposited between Mable Falls Limestone and Viola unconformity and separated by the Forestburg Limestone into Upper Barnett and Lower Barnett. The Viola and Forestburg formations are not producible and provide barriers to fault and fracture growth. Fig. 5 shows the seismic data and the interpreted Upper Barnett Shale and Lower Barnett Shale tops.

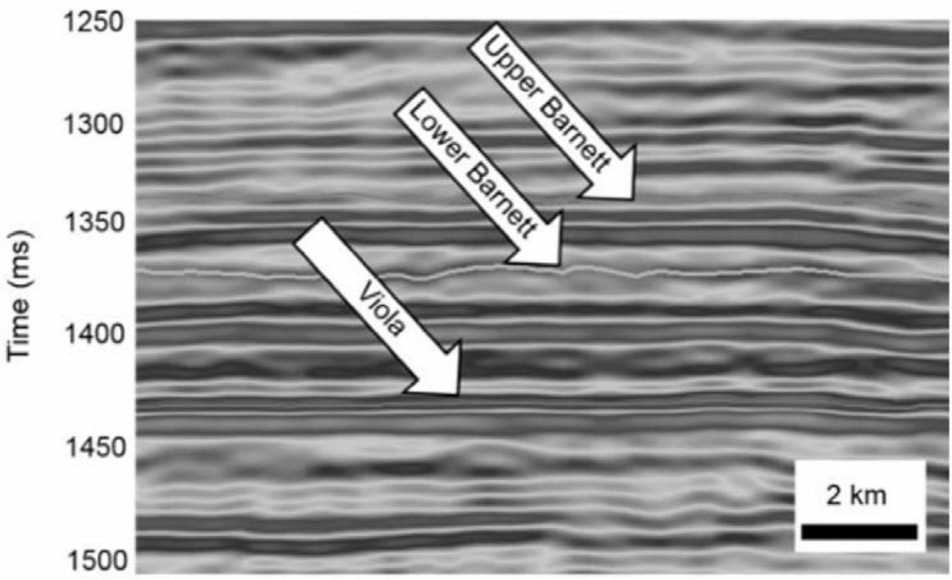

Fig. 5. Seismic data and interpreted horizons tops.

Figs. 6 and 7 show the time structure map and curvature attributes of the Lower Barnett Shale. Seismic attributes show great promise in delineating fracture systems (Chopra and Marfurt, 2008), and has proven to be successful. From Fig. 7, because the fracture scale is below the seismic resolution, we can just infer the potential fracture densities, which should be larger along the natural faults and smaller at others positions.

Then, we applied the CFS method to estimate the Q value, as shown in Fig. 8, in which attenuation means 1/Q. This result has high correspondence with attributes in Fig. 7 and the production data (productive well locations, shown as black circles). Almost all the well locations show high attenuation. More interesting, this result also displays high correspondence with the TOC prediction by Verma et al. (2012). However, we are still surprised by the amount of unphysical negative Q values on the result.

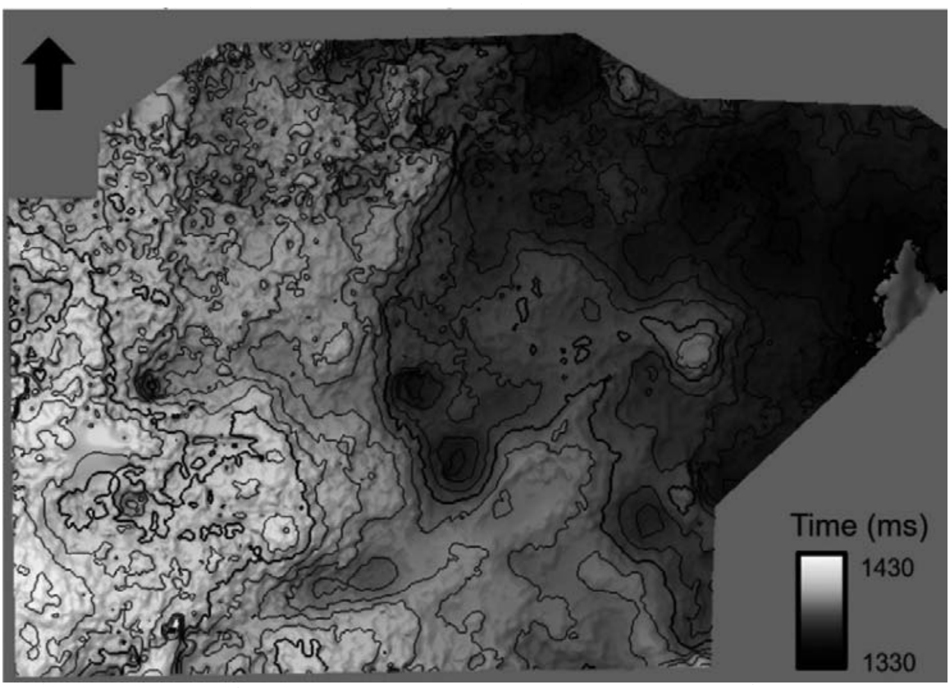

Fig. 6. Time structure map of Lower Barnett Shale.

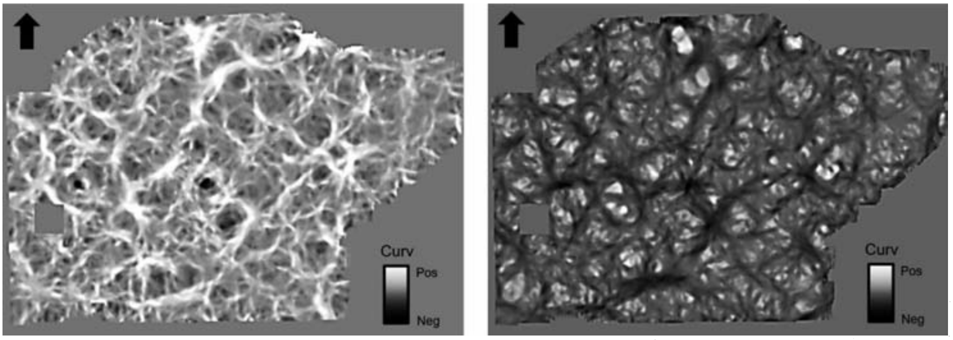

Fig. 7. Attributes horizon slices from Lower Barnett Shale with (left) most positive curvature, (right) most negative curvature.

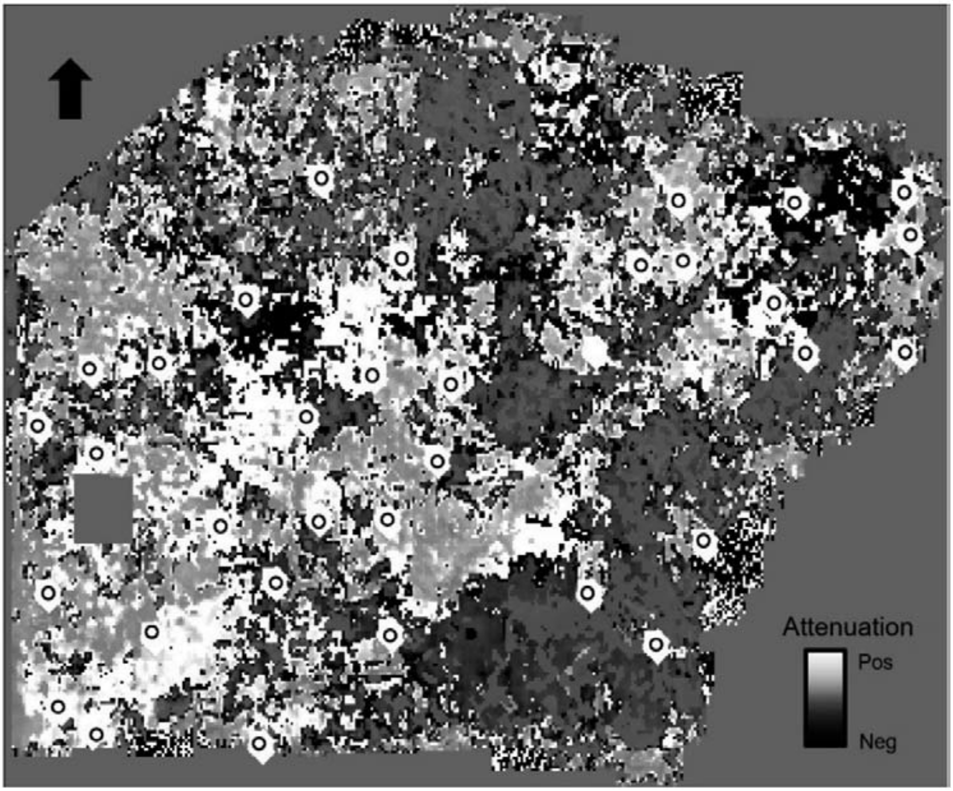

Fig. 8. Attenuation estimation result by CFS method. Black circles denote productive well locations.

In order to eliminate the spectral interference from thin beds, following the workflow in Fig. 1, we perform the Q estimation again. As the reference and target reflections are already picked, first, we need to invert the seismic impedance volume based on well logs (e.g., density and V_P). Fig. 9 shows two well log examples, in which we can find clear thin beds and the reflectivity is certainly not random, which means the spectral correction is really valuable. Fig. 10 displays an inverted seismic impedance section along an arbitrary line, from which the thin-bed layering phenomenon can be observed clearly.

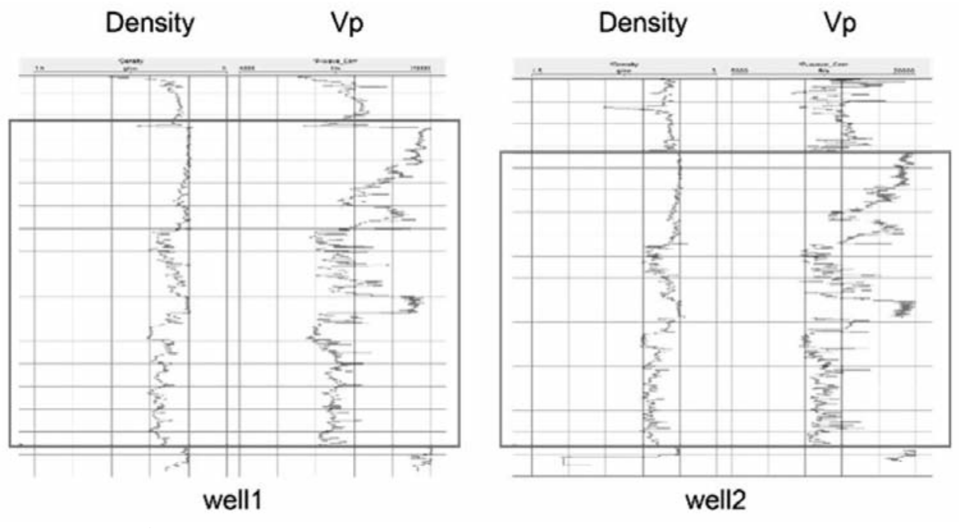

Fig. 9. Well log examples in the survey. Black boxes denote the range of the Lower Barnett Shale, which does not have a white spectrum.

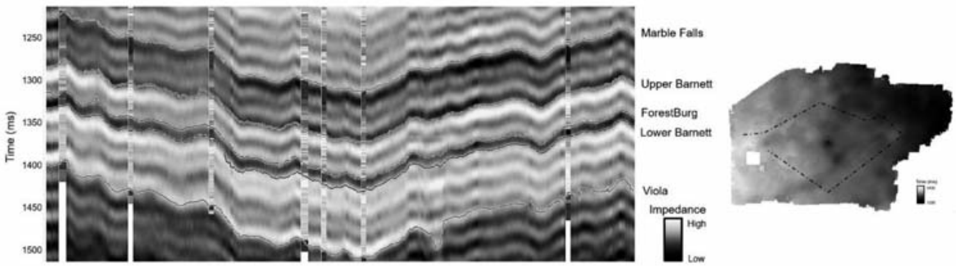

Fig. 10. Inverted seismic impedance profile along an arbitrary line shown on the right. Note the inverted result has a good correspondence with the well logs.

Fig. 11 shows the improved attenuation estimation result. Compared to Fig. 8, upper left area of Fig. 11 has more positive Q values, which makes more sense. But for the bottom right area, there are still many negative values. Comparing the left and right parts of Fig. 10, we note that on the left, only single thin bed shows up, but on the right there are multiple thin beds. In our opinion, the multiple thin beds produce a complicated spectrum, which makes single spectral correction insufficient to remove all the thin bed interference. What would help, is to do the spectral corrections according to the thin beds, which requires accurate thin bed characterization.

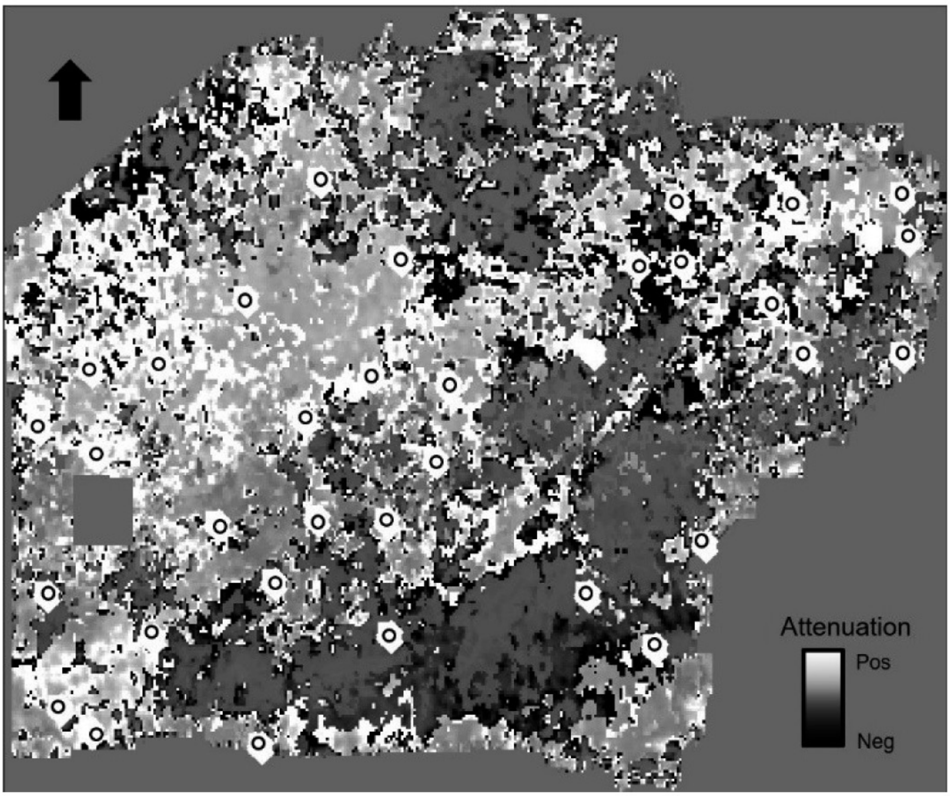

Fig. 11. Attenuation estimation result on corrected data by the CFS method. Black circles denote productive well locations.

CONCLUSIONS

The current "Constant Q" model is inadequate to describe attenuation caused by fracture system in unconventional reservoirs. Reflected wavelets can be distorted by the thin beds, which makes it more difficult to estimate reliable attenuation information. Based on non-stationary convolution model, we demonstrated the successful use of a spectral correction method for improving Q estimation. We applied the method on synthetic examples, and Q values computed using the corrected spectra have less variance and fewer negative values than those computed with uncorrected spectra.

Using the local corrected spectra of the target and reference reflections, we compute Q of the Barnett Shale using the centroid frequency shift (CFS) method. The recovered Q estimates have a good correspondence with the production data, and more physical positive Q values. With the comparison between the results we obtained and the attributes associated with fracture delineation, we can determine that the estimation of seismic attenuation can be a useful tool to evaluate the fracture density, when the valuable information from the well log tied to the seismic data is adopted appropriately.

ACKNOWLEDGEMENTS

Financial support for this effort was provided by the industry sponsors of the Attribute-Assisted Seismic Processing and Interpretation (AASPI) consortium. We thank the State Key Laboratory of Oil and Gas Reservoir Geology and Exploitation in Chengdu University of Technology of China for the partial financial support. The second author (corresponding author) also appreciates Science and Technology Support Program (2011GZ0244) from Science and Technology Department of Sichuan Province of China as well as Chinese Scholarship Council for their support. Special thanks to Devon Energy for providing the seismic and well data over the Barnett Shale for academic research purpose Thanks to CGG GeoSoftware for providing Hampson-Russell software used in seismic inversion.

REFERENCES

Burns, D., Willis, M.E., Minsley, B. and Toksöz, M.N., 2004. Characterizing subsurface fractures from reflected and scattered seismic energy. 112th SEGJ Conf., Tokyo.

Chopra, S. and Marfurt, K.J., 2008. Emerging and future trends in seismic attributes. TLE, 27: 298-318.

Dasgupta, R. and Clark, R.A., 1998. Estimation of Q from surface seismic reflection data. Geophysics, 63: 2120-2128.

Grossman, J.P., Margrave, G.F., Lamoureux, M.P. and Aggarwala, R., 2001. Constant-Q wavelet estimation via a nonstationary Gabor spectral model. Techn. Rep., CREWES, Univ. of Calgary, Calgary, Alberta.

Hackert, C.L. and Parra, J.O., 2004. Improving Q estimates from seismic reflection data using well-log-based localized spectral correction. Geophysics, 69: 1521-1529.

Hauge, P.S., 1981. Measurements of attenuation from vertical seismic profiles. Geophysics, 46: 1548-1558.

Lynn, H. and Beckham, W., 1998. P-wave azimuthal variations in attenuation, amplitude and velocity in 3D field data: Implications for mapping horizontal permeability anisotropy. Expanded Abstr., 68th Ann. Internat. SEG Mtg., New Orleans: 193-196.

Lynn, H., Lynn, W., Obilo, J. and Agarwal, V., 2015. Azimuthal pre-stack depth migration for in-situ stress evaluation in a fractured carbonate oil reservoir: predrill prediction of Instantaneous Shut-In Pressure gradients: GSOC talk.

Pérez, R., 2009. Quantitative petrophysical characterization of the Barnett shale in Newark east field, Fort Worth Basin. M.Sc. thesis, University of Oklahoma, Norman, OK.

Quan, Y. and Harris, J.M., 1995. Seismic attenuation tomography using the frequency shift method. Geophysics, 62: 895-905.

Sheriff, R.E. and Geldart, L.P., 1995. Exploration Seismology, 2nd ed., Cambridge University Press, Cambridge.

Verma, S., Roy, A., Perez, R. and Marfurt, K.J., 2012. Mapping high frackability and high TOC zones in the Barnett Shale: supervised probabilistic neural network vs. unsupervised multi-attribute Kohonen SOM. Expanded Abstr., 82nd Ann. Internat. SEG Mtg., Las Vegas.

White, R.E., 1992. The accuracy of estimating Q from seismic data. Geophysics, 57: 1508-1511.

Zhang, C.J. and Ulrych, T.J., 2002. Estimation of quality factors from CMP records. Geophysics, 67: 1542-1547.